Final Draft
of the original manuscript:

Xu, X.; Kratz, K.; Wang, W.; Li, Z.; Roch, T.; Jung, F.; Lendlein, A.; Ma, N.:
Cultivation and spontaneous differentiation of rat bone marrow-derived mesenchymal stem cells on polymeric surfaces
In: Clinical Hemorheology and Microcirculation (2013) IOS Press

DOI: 10.3233/CH-131698

Cultivation and spontaneous differentiation of rat bone marrow-derived mesenchymal stem cells on polymeric surfaces

Xun Xu[#], Karl Kratz[#], Weiwei Wang[#], Zhengdong Li, Toralf Roch, Friedrich Jung, Andreas Lendlein* and Nan Ma[#]

Institute of Biomaterial Science and Berlin-Brandenburg Centre for Regenerative Therapies, Helmholtz-Zentrum Geesthacht, Teltow, Germany

[#] Xun Xu, Karl Kratz, Weiwei Wang, Nan Ma contributed equally to this work.

***Correspondence:**

Prof. Dr. Andreas Lendlein
Institute of Biomaterial Science and Berlin-Brandenburg Centre for Regenerative Therapies, Helmholtz-Zentrum Geesthacht, Kantstr. 55, 14513 Teltow, Germany

Email: andreas.lendlein@hzg.de
Phone: +49 (0)3328 352-450
Fax: +49 (0)3328 352-452

Abstract:

Accumulating evidence demonstrated many physical and chemical cues from the local microenvironment could influence mesenchymal stem cells (MSCs) maintenance and differentiation. In this study, we systematically investigated the interaction of rat bone marrow-derived mesenchymal stem cells (rBMSCs) and polymeric substrates. Adhesion, proliferative capacity, cytoskeleton alteration, cytotoxicity, apoptosis, senescence, and adipogenesis potential of rBMSCs were determined on these polymeric inserts prepared from polyetherurethane (PEU) and poly(ether imide) (PEI). Inserts for culture plates were applied to ensure that the rBMSCs were solely in contact to the tested material. The explored inserts exhibited advancing contact angles of 84° (PEU) and 93° (PEI). Finally, the micromechanical properties determined by atomic force microscopy (AFM) indentation varied in the range from 6 GPa (PEU) to 13 GPa (PEI). We found that both PEU and PEI showed a good cell compatibility to rBMSCs. rBMSCs could adherent on both polymeric surfaces with the similar adhesion ratio and subsequent division rate. However, cells cultured on PEU exhibited higher apoptosis level and senescence ratio, which resulted in lower cell density (22061±3000/cm^2) compared to that on PEI (68395±8000/cm^2) after 20 days cultivation. Morphological differences of rBMSCs were detected after 5 days cultivation. Cells on PEU exhibited flat and enlarged shape with rearranged filamentous actin (F-actin) cytoskeleton, while cells on PEI and tissue culture plate (TCP) had similar spindle-shape morphology and oriented F-actin. After 20 days, lipid droplets were spontaneously formed in rBMSCs on PEU and PEI but not on TCP. Both PEU and PEI might trigger rBMSCs towards spontaneous adipogenic commitment, whereas PEI provided better cell compatibility on rBMSCs apoptosis, senescence and proliferation.

Keywords: Mesenchymal stem cells, polymeric surface, cell-material interaction, cellular senescence, spontaneous differentiation

1 Introduction

Cell transplantation utilizing various cell types has emerged as a promising therapeutic approach for restoration of organ functions. Among these investigated cells, mesenchymal stem cells (MSCs) attracted a lot of attention [26, 34, 36, 45], since they are self-renewing clonal precursors of non-hematopoietic stromal tissues and could differentiate into specific lineages including osteoblasts, chondrocytes and adipocytes under appropriate environment or inductions [28, 35, 38, 44]. However, the unexpected low cellular engraftment after transplantation greatly limited their clinical translation. Similar as other somatic cells, MSCs also undergo the typical "Hayflick limit" and show the cellular senescence phenotypes [42]. It has been speculated that the replicative senescence could be triggered by accumulation of cellular defects, changes of telomeres or telomerase and the external culture environments such as oxidative stress [23, 43]. In addition, the specific surface features may also influence the self-renewal and senescence of stem cells. The senescence could lead to alternation in gene expression of molecular signature and decline of cell functions [6, 30]. Thus, it is necessary to combine MSCs with biomaterials to establish an optimized condition for MSCs maintenance and differentiation and therefore improve the efficacy of cell therapy.

In recent years, several studies have reported the influence of physicochemical properties of cell culture surfaces on the *ex vivo* maintenance and differentiation of MSCs [11, 13, 15, 16], but in most of these investigations, the tested materials were placed in commercially available tissue culture plate (TCP), which might involve the influence of the fixation materials or TCP itself. Here, a recently introduced polymeric insert system for cell culture plates was applied to ensure that the MSCs were solely in contact to the tested material [18]. We selected poly(ether imide) (PEI), a biocompatible polymer, which allows to alter the surface chemistry [3, 18, 24, 40] and an elastic polyetherurethane (PEU), which allows to adjust the mechanical properties by variation of the hard to soft segment ratio and exhibited good biocompatibility and a shape-memory effect, which is of high interest for minimally-invasive applications [8, 22, 25].

In this study, we investigated the self-renewal and spontaneous differentiation of rat bone marrow-derived mesenchymal stem cells (rBMSCs) on PEU and PEI surfaces in comparison to TCP with regard to proliferation, adhesion, cytotoxicity, apoptosis, senescence and morphological changes.

2 Materials and Methods

The study was performed in accordance with the ethical guidelines of the journal Clinical Hemorheology and Microcirculation [1].

2.1 Processing and surface characteristics of the polymeric inserts

PEU with M_n = 61.000 g/mol (trade name Tecoflex® MG8020, Lubrizol, USA) and PEI with M_n = 18.000 g/mol (trade name ULTEM® 1000, General Electric, USA) were used without any further purification for preparation of polymeric inserts via injection moulding. The injection moulding automat (Alrounder 270U, Arburg Corp., Münsingen, Switzerland) was equipped with a custom made mould (Dreuco Formenbau GmbH, Berlin, Germany), allowing the parallel fabrication of four inserts with an upper inner diameter of 12.4 mm, an lower inner diameter of 10.5 mm, a height of 16.8 mm, and a wall thickness of 1 mm. The structural formulas of both polymers are shown in Fig. 1A and the detailed processing parameters are summarized in Table 1. Prior to biological testing and surface characterization of the insert bottom, PEU inserts were sterilized by gas sterilization using ethylene oxide (gas phase: 10% ethylene oxide, 54 °C, 65% relative humidity, 1.7 bar, gas exposure time: 3 h, aeration phase: 21 h) while PEI inserts were sterilized via steam sterilization at 121 °C and a pressure of 2.0 bar for 20 minutes using a Systec Autoclav D-65 (Systec GmbH, Wettenberg, Germany).

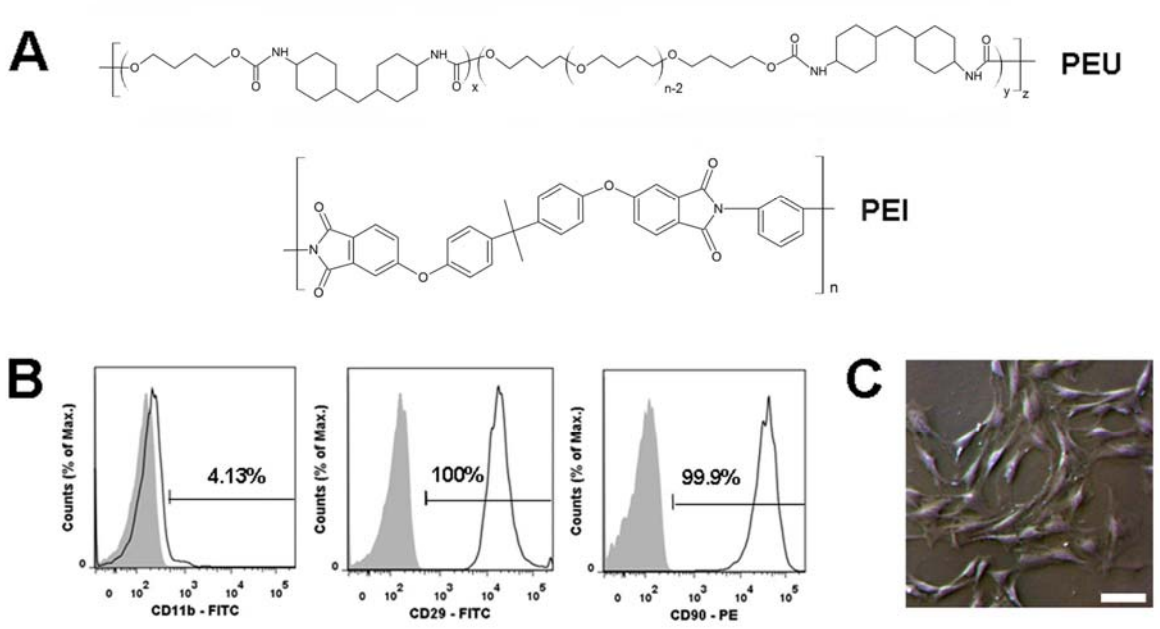

Figure 1. Chemical structures of investigated polymers (A) and characterization of rBMSCs. (B) The flowcytometric analysis of rBMSCs. rBMSCs were stained with monoclonal antibodies against CD29, CD90 and CD11b (solid black line) and appropriate isotype controls (grey filled curve). (C) Typical spindle-shaped morphology of enriched rBMSCs on TCP was observed by phase-contrast microscopy. Scale bar =100 µm.

Table 1. *Processing parameters applied for PEU and PEI*

Polymers	Processing parameter							
	Temperature of melt – four zone heating [°C]				Temperature of mold [°C]	Injection rate – two-stage [cm³/s]	Injection pressure – two-stage [bar]	Injection volume [cm³]
	I	II	III	IV				
PEU	35	150	180	190	20	25-30	1200-1800	6.5
PEI	35	320	350 /360	350 /380	180/140	35-40	1800-2000	11

The surface characteristics of the PEI and PEU inserts were assessed by determination of the water contact angle measurements using the captive bubble method and optical profilometry. Both inserts exhibited an almost similar wettability with advancing contact angles of 84° for PEU and 93° for PEI. While PEI showed a surface roughness (R_q) of R = 0.23 µm and for PEU a higher R = 0.86 µm was observed. In addition, the micromechanical characterization of the insert bottom was conducted at ambient temperature with an atomic force microscope (AFM) equipped with an indenter. Here a Young´s modulus of 6 GPa was determined by microindentation for PEU, while PEI exhibited a significant higher value of 13 GPa. The lower Young´s modulus as well as the higher surface roughness of PEU can be attributed to the relatively low and broad mixed glass transition of PEU in the range from 20 °C to 90 °C, which allow relaxation of the polymer chains at ambient temperature [8, 22].

2.2 Culture and characterization of rBMSCs

rBMSCs were kindly provided by Dr. Jun Li (University of Rostock, Germany. Approval number: LALLF M-V/TSD/7221.3-2.3-019/07), which were isolated from rat bone marrow from Lewis rat as described previously [14]. Dulbecco's modified Eagle's medium (Life Technologies GmbH, Germany) supplemented with 10% fetal bovine serum (Biochrom AG, Berlin, Germany) and 10 U/mL penicillin plus 100 µg/mL streptomycin was used as expansion medium for culturing cells at 37 °C in a humidified atmosphere containing 5% CO_2.

The cells from passage 3 were used for experiments. The morphology of cells was observed by inverted phase contrast microscope (Axiovert 40c, Carl Zeiss GmbH, Germany). The surface marker expression of rBMSCs was examined by flow cytometry (MACSQuant® Analyzer, Miltenyi Biotec, Germany). The following cell-surface epitopes were stained with following antibodies: anti-rat CD29-FITC, CD11b-FITC and CD90-PE (BD Biosciences, Heidelberg, Germany). Mouse and hamster isotype antibodies served as control. For each flow cytometric running, 1.5×10^4 labeled cells were acquired and the data were analyzed using "Flowjo" software (v7.6.1, Tree Star Inc., USA).

2.3 Cell growth on polymeric surfaces

rBMSCs expansion on polymeric surfaces was evaluated using Cell Counting kit-8 (CCK-8, Dojindo Laboratories, Kumamoto, Japan) according to the product manual. TCP was applied as a positive control. Briefly, cells were seeded at a density of $1.0\times10^4/cm^2$ in polymeric inserts and 24-well culture plates (Corning Costar®, Corning Life Sciences, USA). The culture medium was changed regularly at a volume of 300 $\mu L/cm^2$ of culture area. On days 1, 5 and 20 post cell-seeding, the soluble monosodium salt from CCK-8 kit was added to the culture medium (33 $\mu L/cm^2$). After 2.5 hours of incubation at 37 °C, the water soluble formazan dye with a yellow colour was produced. 100 µL of supernatant from each sample was taken into 96-well plate with a clear flat bottom and the absorbance was measured at 490 nm (reference wavelength: 650 nm) by using Tecan Infinite® 200 PRO microplate reader (Tecan Deutschland GmbH, Germany). The experiment was performed at least in triplicates.

2.3.1 Cell division

3×10^5 rBMSCs were suspended in phosphate buffered saline (PBS) and labeled with 20 µM carboxyfluorescein diacetate succinimidyl ester (CFDA-SE) for 15 minutes at 37 °C. Then, the cells were washed twice with PBS and subsequently seeded into the inserts and TCP at a cell density of 1.0×10^4 cells/cm^2. The non-fluorescent dye CFDA-SE is cleaved by intracellular to carboxyfluorescein succinimidyl ester (CFSE) esterase and irreversibly couples to amines to form fluorescent conjugates. The fluorescent CFSE-conjugates are distributed equally between daughter cells. The reduction of CFSE mean fluorescence intensity (MFI) due to the division of the cells was assessed by flow cytometry (MACSQuant® Analyzer, Miltenyi Biotec, Germany) and the data were analyzed by using Flowjo software (v7.6.1, Tree Star Inc., USA).

2.3.2 Cytotoxicity assay

Cell viability staining was performed using fluorescein diacetate (FDA) and propidium iodide (PI) (Sigma Aldrich Chemie GmbH, Germany). In brief, on day 1, 5 and 20 after cell-seeding (1×10^4 cells/cm^2), FDA (25 µg/mL) and PI (2 µg/mL) were directly added to the cells and incubated for 3 minutes at 37 °C. A confocal laser scanning microscope (LSM 510 META with the AxioVision image analysis software v4.2, Carl Zeiss GmbH, Germany) was utilized to observe the stained cells. Cells cultured in TCP were used as control.

2.4 Cytoskeleton staining

On day 5 after cell-seeding (1×10^4 cells/cm^2), cells were fixed with 4% (w/v) paraformaldehyde and permeabilized by 0.3% (v/v) Triton® X-100 (both from Sigma Aldrich Chemie GmbH, Germany), followed by a staining of filamentous actin (F-actin) by rhodamine conjugated phalloidin (6.6 nM; Life Technologies GmbH, Germany). Each experiment was conducted in duplicates.

2.5 Apoptosis assay

ApoLive-Glo™ Multiplex Assay Kit (Promega GmbH, Germany) was used for determination of early apoptotic rBMSCs. Cells were cultured in inserts and TCP for growing. On day 1, 5 and 20 post cell-seeding, cells were harvested and reseeded (100 µL per well, duplicate for each sample) in Nunc™ F96 MicroWell™ 96-well solid-bottom black plates (Thermo Electron LED GmbH, Germany) to perform apoptosis assay. Following the product manual, 20 µL of Viability Reagent were added to each well, and briefly mixed by orbital shaking at 500 rpm for 30 seconds. The mixture was subsequently incubated for 1 hour at 37 °C. The relative fluorescence units (RFU) from viable cells were measured at the following wavelength of 400 nm (excitation) /505 nm (emission). Then 100 µl of Caspase-Glo® 3/7 Reagent were directly added to each well, and briefly mixed at 500 rpm for 30 seconds. After another 2 hours of incubation at room temperature in dark, the Caspase-3/7 activation was determined by measuring the relative light units (RLU) of the luminescence intensity. Both fluorescence and luminescence were measured by Tecan Infinite® 200 PRO microplate reader (Tecan Deutschland GmbH, Germany). Duplicate samples containing only culture medium were served as the negative control for background subtraction.

2.6 SA beta-gal activity assay

Senescence Cells Histochemical Staining Kit (Sigma Aldrich Chemie GmbH, Germany) was used to identify senescent cells with a rapid staining procedure for detecting senescence-associated beta-galactosidase (SA beta-gal) activity at pH 6. In brief, on day 5 and 20, the growth medium from inserts and TCP was aspirated and the cells were washed twice with PBS. rBMSCs were fixed by adding 1×Fixation Buffer (300 μL/well) and incubating for 7 minutes at room temperature. Subsequently, these cells were rinsed 3 times with PBS and stained by Staining Mixture (200 μL/well) overnight at 37 °C at the absence of CO_2 until the senescent cells became cyan. The numbers of senescent cells and the total cells were counted at four different fields of view under a microscope (Axiovert 40c, Carl Zeiss GmbH, Germany), and the senescence ratio was expressed as the percentage of the number of senescent cells out of the number of total cells.

2.7 Detection of morphological change

To further study the morphological change of the cells after a period of culture, the cells were seeded in polymeric inserts and TCP and the expansion media were changed regularly. After 20 days of culture, the morphology of cells was recorded by inverted phase contrast microscope (Axiovert 40c, Carl Zeiss GmbH, Germany).

2.8 Statistics

Data were presented as mean value ± standard deviation (Mean ± SD), and were statistically analyzed by two-tailed independent samples *t*-test. A p value less than 0.05 was considered to be statistically significant.

3 Results

3.1 Cell characterization

To characterize rBMSCs, their phenotype was examined via flow cytometry. rBMSCs were positive for CD29, CD90 and devoid of hematopoietic marker CD11b. All rBMSCs expressed CD29 and 99.9% expressed CD90, while only 4.13% expressed CD11b (Fig. 1B). The cultured rBMSCs displayed a typical spindle-shaped morphology (Fig. 1C).

3.2 Cell adhesion, expansion and division

The cells could adhere to PEU, PEI and TCP surfaces, and then divide and expand. By dividing the number of the adherent cells with the number of seeded cells, the cell adhesion rate could be calculated. 24 hours after cell-seeding, the cell adhesion rate was 44±9% (PEU), 45±2% (PEI) and 80±4% (TCP), respectively (Fig. 2A). The adherent cells proliferated on PEU, PEI and TCP surfaces. The MFI of CFSE of the cells on PEU, PEI and TCP exhibited a similar trend, indicating the similar division rate of the cells on these three different surfaces (Fig. 2B). However, the numbers of cells on PEU, PEI and TCP measured via CCK-8 exhibited a remarkable difference (Fig. 2A). Cells growing on PEU showed the lowest proliferation rate, whose value was statistically lower than that on PEI and TCP, after both short-term (5 days) and long-term (20 days) cultivation. Although the cell number on PEI was statistically lower than that on TCP at early stage (5 days), it achieved a comparable level to that on TCP at day 20, indicating that PEI possesses the excellent biocompatibility for rBMSCs expansion. After 20 days cultivation, the cell density reached to 22061±3000/cm^2 (PEU) and 68395±8000/cm^2 (PEI) respectively, resulting in the fold change of 5.0 and 15.1 compared to the number of attached cells (Fig. 2A).

3.3 Cell viability

In order to determine the viability of rBMSCs growing on the polymeric surface, cells were stained by fluorescent dyes FDA and PI (Fig. 2C). We found that the polymeric surfaces exhibited low cytotoxicity and allowed high cell viability in a time-independent way. As a result, the low death rate of cells cultured in PEU and PEI inserts was observed from 1 to 20 days cultivation time. The polymeric inserts did not show obvious differences to TCP with respect to cytotoxicity and viability.

3.4 Morphological study

On PEU, the spread out, flat enlarged cell shape of rBMSCs was observed, whereas on other surfaces the typical spindle shapes were exhibited at day 5 of cultivation (Fig. 3A). The F-actin cytoskeleton structures were stained as described in the Materials and Methods section.

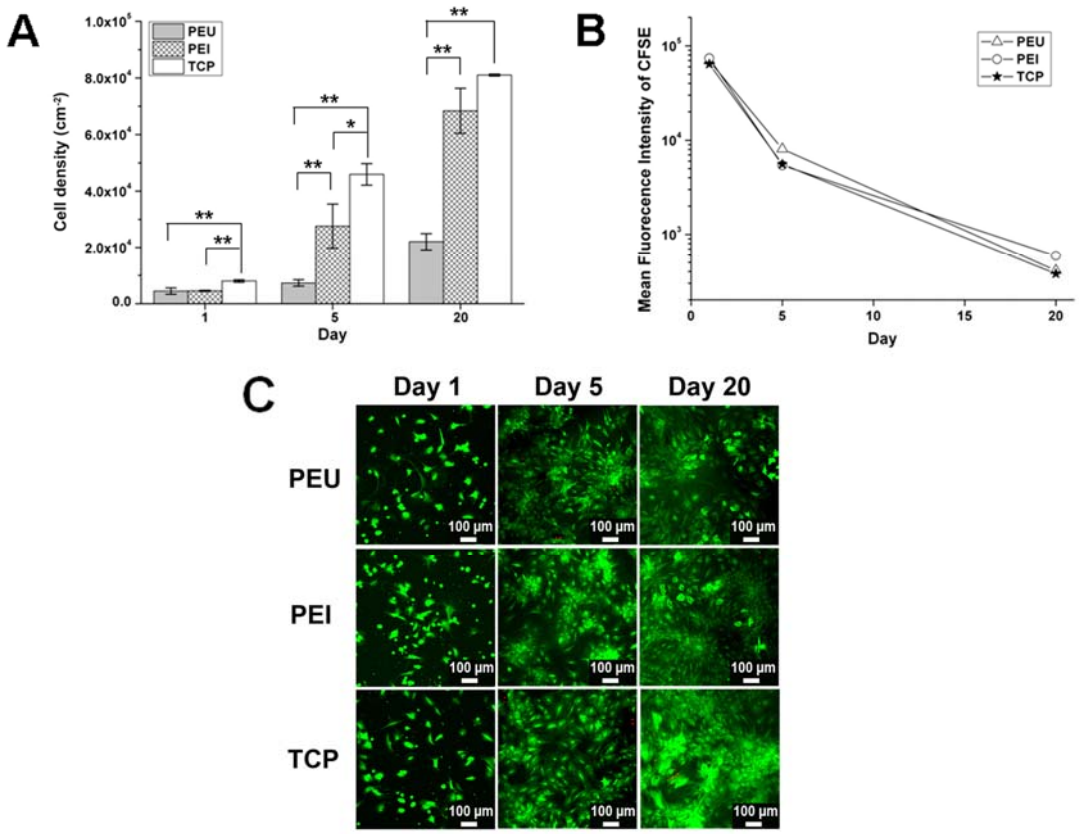

Figure 2. Expansion and viability of rBMSCs on polymeric surfaces. *(A) Expansion of rBMSCs cultured on PEU, PEI and TCP (Mean ± SD, n=3, * p<0.05, ** p<0.01 by independent samples t test). (B) rBMSCs division was analyzed by CFSE tracking. MFI values of CFSE at different time points of rBMSCs cultivation were calculated by Flowjo software. (C) Fluorescent images of rBMSCs stained by FDA (green)-PI (red). Few dead cells (around 0-4) were observed in one high-power field. Scale bar =100 µm.*

At 5 days cultivation time, cells growing on both PEI and TCP surfaces showed the similar stress fibers distribution, which aligned on the long-axis of cells. In contrast, on the surface of PEU, predominantly random stress fiber orientation was visualized, which may relate to the low glass transition temperature of PEU and more randomly orientated macromolecules (Fig. 3B).

3.5 Level of apoptotic cells

ApoLive-Glo™ multiplex assay kit was used for detecting caspase-3/7 activation, which is a key biomarker of early apoptosis. The apoptosis level was expressed as the luminescence intensity (RLU) of Caspase-3/7 activation normalized by the fluorescence intensity (RFU) from viable cells.

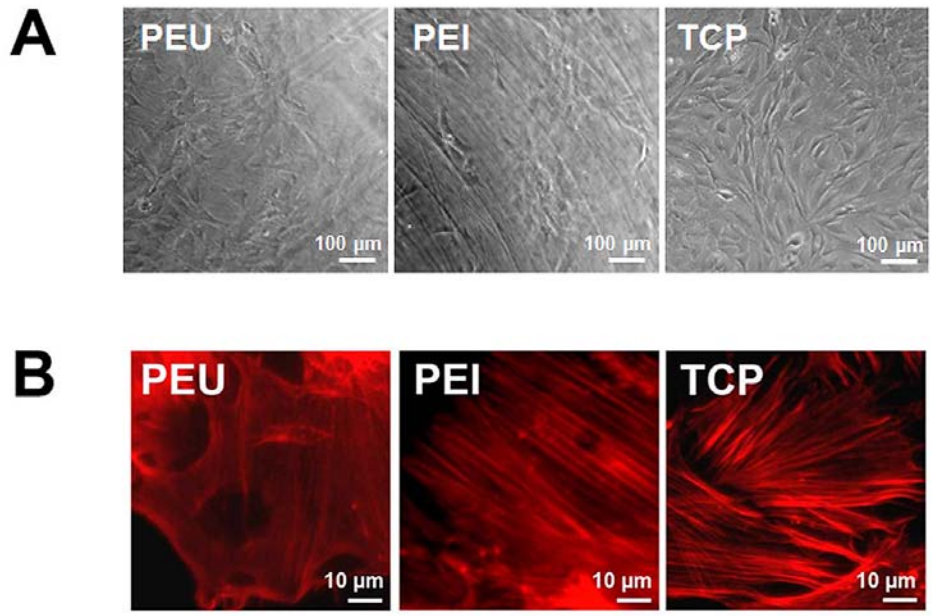

Figure 3. Morphology of rBMSCs on PEU, PEI and TCP. *(A) Phase contrast microscopic images and (B) fluorescent microscopic images showing F-actin cytoskeleton of rBMSCs cultured on PEU, PEI and TCP at 5 days cultivation time. (Upper panel: scale bar=100µm and lower panel: scale bar=10µm, respectively)*

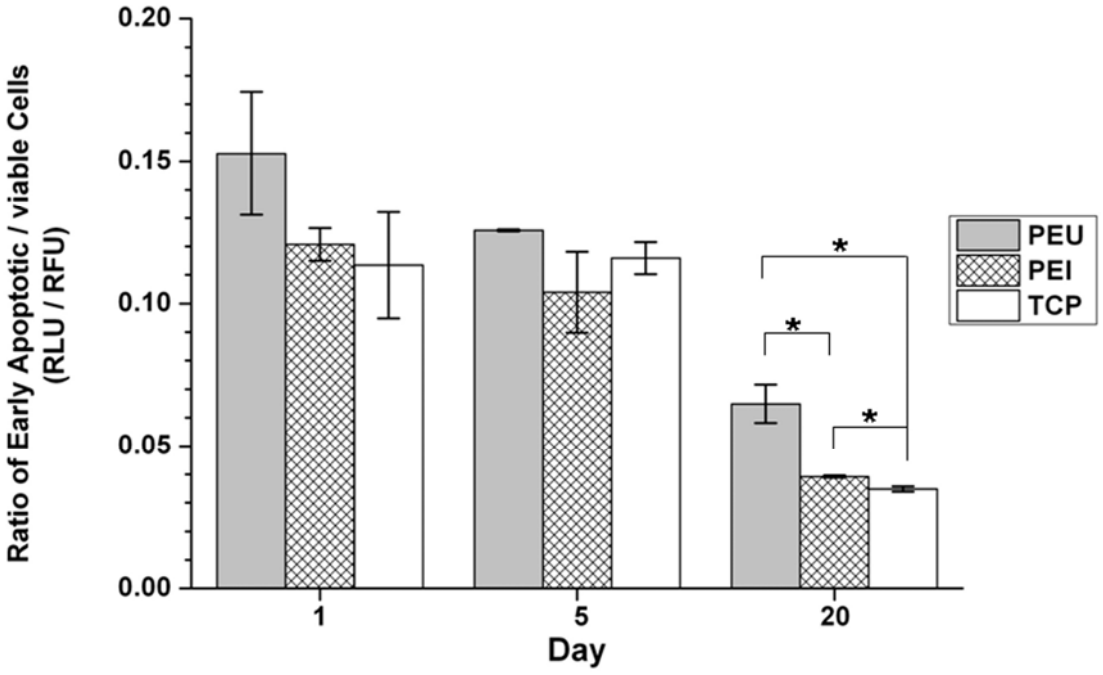

Figure 4. Analysis of caspase 3/7 activation-based apoptosis. *Levels of apoptotic rBMSCs were measured at different time points on PEU, PEI inserts as well as TCP. RLU from apoptotic cells was normalized with RFU from viable cells. (Mean ± SD, n=2, * p<0.05, by independent samples t test)*

During a 20 days cultivation time period, with the increase of time, the apoptosis levels of rBMSCs were dramatically decreased for all tested contact surfaces. There were no significant differences in apoptosis level between PEU, PEI and TCP group at day 1 and day 5. At day 20 of cultivation, the apoptosis level of rBMSCs on PEI and TCP was significantly lower compared to PEU (Fig. 4).

3.6 Ratio of senescent cells

To access the senescence level, we analyzed SA beta-gal expression in rBMSCs cultured on different polymeric surfaces. We found that the polymers induced the cell senescence in a time-independent manner, since no significant changes of senescence rate between day 5 and day 20 of cultivation were observed. The percentage of beta-gal positive rBMSCs on PEU surface was higher compared to those on PEI and TCP (Fig. 5A, Fig. 5B). These results suggest that in contrast to PEI, PEU might induce SA beta-gal up-regulation of rBMSCs and maintain it at the high level.

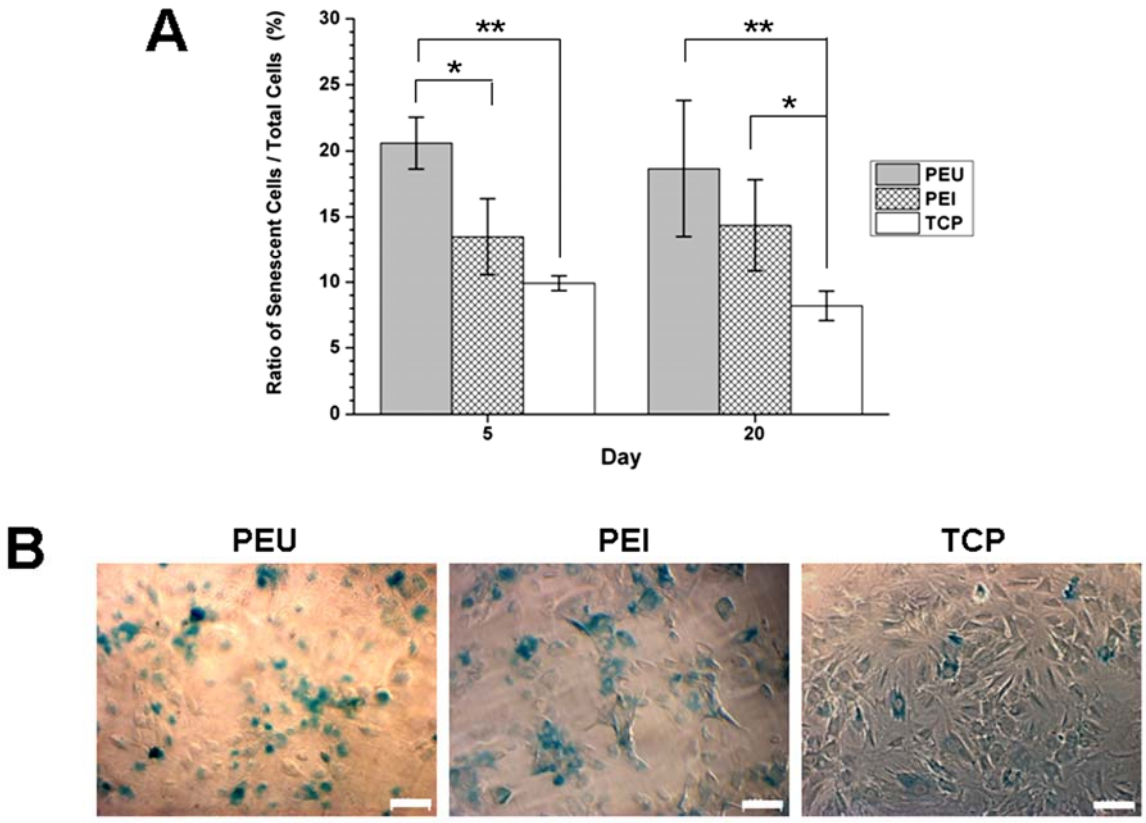

Figure 5. Effect of different polymeric surfaces on rBMSCs cellular senescence. *SA beta-gal assay was performed on rBMSCs. (A) The number of cyan stained SA beta-gal-positive cells and total cells were counted at four different fields of view. The result was expressed as the percentage of the number of senescent cells out of the number of total cells (Mean ± SD, n=4, * p<0.05, ** p<0.01 by independent samples t test). (B) Representative photographs of SA beta-gal staining of cells on PEU, PEI and TCP at pH 6. Scale bar =100 µm.*

3.7 Spontaneous adipogenic differentiation

Without any additional differentiation stimuli, after 20 days of cultivation, cells' growing in polymeric inserts and TCP exhibited different morphologies. rBMSCs cultured in TCP showed a typical spindle-like shape, whereas lipid droplets were found in numerous cells in both polymeric inserts (Fig. 6). The morphological change indicated that the rBMSCs differentiated towards adipogenic lineage.

4 Discussion

MSCs offer tremendous potential for regenerative medicine [41]. However, MSCs could only be expanded *ex vivo* to a certain passage. Then the cells will go through growth arrest and replicative aging. The long term expansion of MSCs is still an unrealized challenge. Plasma treated polystyrene is widely used as cell culture plate material, which is poorly resistant to some organic solvents and is fragile. Recent developments in the field of biomaterials can provide a powerful approach to maintain the MSCs phenotype, stemness and multipotency in the absence of complex growth factors [32].

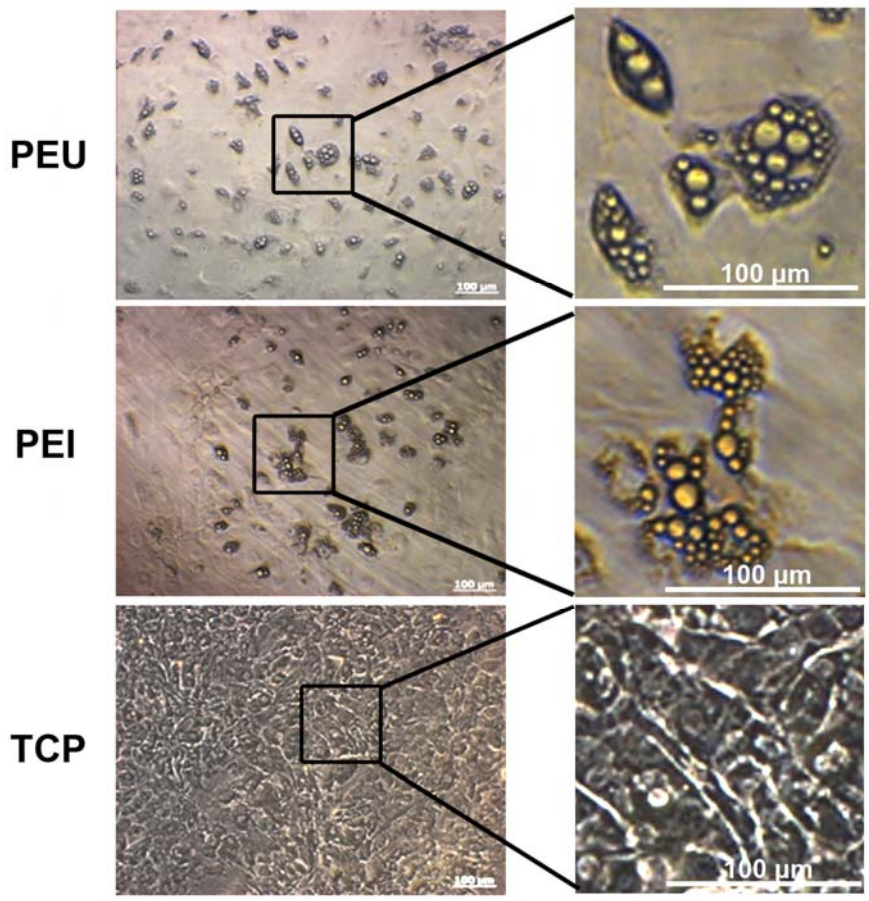

Figure 6. Spontaneous morphological change of rBMSCs. *After 20 days of cultivation, no spontaneous morphological change of cells occurred on TCP. However, the formation of lipid droplets was observed by phase-contrast microscopy for cells cultured on PEU and PEI. Scale bar =100 µm.*

The appropriate chemical signals and/or physical features of the surface could influence the cell behaviour and may modulate cell aging [21, 37]. In our present study, we employed polymeric inserts prepared from PEU and PEI for the assessment of the interaction between rBMSCs and the polymer surfaces.

rBMSCs could be expanded on both PEU and PEI surfaces, which exhibited a remarkably low cytotoxicity. Nevertheless, different responses of rBMSCs on the two types of polymeric surfaces were detected. A lower expansion rate and a higher apoptosis level of rBMSCs were found on PEU surface compared to PEI. We also observed a remarkable alteration of morphology, cytoskeleton reorganization and high enzymatic SA beta-gal activity of cells on PEU, which may be associated with senescence. Furthermore, both polymers could induce spontaneous adipogenesis of rBMSCs. Based on our findings, PEI might be considered as a better polymer for rBMSCs cultivation with lower senescence ratio and apoptosis level.

Hayflick and Moorhead discovered that human diploid fibroblasts could only have a limited ability to divide and then enter a growth arrest [17]. Like other somatic cells, MSCs also undergo the replicative senescence, which may be characterized by morphological change with spread out, flat enlarged cell shape and up-regulation of SA beta-gal [2, 4, 10, 20, 42, 46]. There are many possible reasons for cell senescence including chemical signals and physical features. It was reported that hydrophilic polymeric surface could accelerate the fibroblast cell aging [27]. However, in our study there was no statistical difference on hydrophilicity between PEI and PEU surface. We speculate that MSCs senescence, as a reflection of the local environment or culture stress, may be associated to the cultivation microenvironment including the chemical structure of the polymer. Different chemical composition may induce different absorption of proteins, particular elements of ECM, which may either trigger or delay the aging process. To identify the possible reasons is a very interesting topic but beyond the scope of this study.

Both polymeric surfaces had similar cell initial adhesion and division rate. However, the cell density on PEU was much lower than that on PEI surfaces after 20 days cultivation. This discrepancy may be attributed to the higher apoptosis and senescence on PEU. This finding was in agreement with previous studies, in which the proliferation rate of MSCs has a negative correlation with cell senescence and apoptosis [2, 7, 29, 39]. Therefore, we believe it will be of great importance to monitor the apoptosis level and senescence ratio as crucial parameters to study cell-material interaction.

Accumulating evidence indicates that MSCs are highly sensitive to their local environments and their linage commitment could be regulated by many cues provided by chemistry [31], stiffness [19], and topography [9]. Interestingly, we found the formation of numerous nascent lipid droplets in rBMSCs on PEI and PEU surface, which indicates the early adipogenic differentiation without any additional induction. Previous studies have suggested that adipogenesis could be triggered by high cell density and cytoskeleton reorganization [4, 5, 20, 31, 46]. In the present study, the high cell density was excluded as the possible reason for adipogenesis since on both PEU and PEI surfaces the cell densities were sparse and lower than that on TCP when the differentiation occurred. The morphological change might be one of the factors for driving the spontaneous differentiation. It was suggested that cell shape might regulate the dedicated adipogenic/osteogenic MSCs fate decisions [5, 31]. The different cytoskeleton rearrangement might influence the cell spreading and cellular conformation, the signal of which could be further transferred into the nucleus and alter the gene transcription of cells, which might result in the outcome of spontaneous adipogenesis [12]. Furthermore, we also found that there were high levels of both senescent and adipogenic differentiated cells on PEU and PEI surfaces. The soluble factors, which have been secreted from the senescent cells, may also alter the local environment and elicit the spontaneous adipogenic commitment [33]. In addition, the different chemical composition of cell culture surfaces may play a role for the adipogenic differentiation, which needs to be further clarified and protein adsorption on the polymeric surfaces should be investigated as well.

5 Conclusions

In this study, we compared the influences of PEU and PEI on rBMSCs with respect to cell adhesion, proliferation, cytoskeleton reorganization, cytotoxicity, apoptosis, senescence and differentiation potential. Our results demonstrated that both tested polymeric surfaces were compatible for rBMSCs cultivation. PEI was the better suitable surface for rBMSCs expansion with a low senescence ratio and apoptosis level. Both PEU and PEI surfaces promoted a spontaneous adipogenic commitment, which may be attributed to morphological change of cells and chemical composition of the polymeric surfaces. The underline mechanism of spontaneous differentiation without any induction should be further clarified. Moreover, it is of great importance to employ the chemical and physical characters of biomaterials to influence the stem cell fate decision in cell therapy.

Acknowledgements

The authors thank the Bundesministerium für Bildung und Forschung (BMBF project number 0315696A 'Poly4Bio BB') and Helmholtz Association for the financial support, and Ms. Angelika Ritschel, Ms. Ruth Hesse, Ms. Anja Müller-Heyn, Mrs. Manuela Keller, Mr. Robert Jeziorski and Mr. Oliver Frank for their technical assistance.

Competing interests

The authors declare that they have no competing interests.

References

[1] Anonymous, Ethical Guidelines for Publication in Clinical Hemorheology and Microcirculation, *Clinical Hemorheology and Microcirculation*, **44** (2010), 1-2.

[2] M.M. Bonab, K. Alimoghaddam, F. Talebian, S.H. Ghaffari, A. Ghavamzadeh and B. Nikbin, Aging of mesenchymal stem cell in vitro, *BMC Cell Biology*, **7** (2006), 14.

[3] S. Braune, M. Lange, K. Richau, K. Lutzow, T. Weigel, F. Jung and A. Lendlein, Interaction of thrombocytes with poly(ether imide): The influence of processing, *Clinical Hemorheology and Microcirculation*, **46** (2010), 239-250.

[4] S.P. Bruder, N. Jaiswal and S.E. Haynesworth, Growth kinetics, self-renewal, and the osteogenic potential of purified human mesenchymal stem cells during extensive subcultivation and following cryopreservation, *Journal of Cellular Biochemistry*, **64** (1997), 278-294.

[5] L.B. Buravkova, P.M. Gershovich, J.G. Gershovich and A.I. Grigorev, Mechanisms of Gravitational Sensitivity of Osteogenic Precursor Cells, *Acta Naturae*, **2** (2010), 28-36.

[6] Q. Chen, A. Fischer, J.D. Reagan, L.J. Yan and B.N. Ames, Oxidative DNA-Damage and Senescence of Human-Diploid Fibroblast Cells, *Proceedings of the National Academy of Sciences of the United States of America*, **92** (1995), 4337-4341.

[7] V.J. Cristofalo, R.G. Allen, R.J. Pignolo, B.G. Martin and J.C. Beck, Relationship between donor age and the replicative lifespan of human cells in culture: A reevaluation, *Proceedings of the National Academy of Sciences of the United States of America*, **95** (1998), 10614-10619.

[8] J. Cui, K. Kratz, M. Heuchel, B. Hiebl and A. Lendlein, Mechanically active scaffolds from radio-opaque shape-memory polymer-based composites, *Polymers for Advanced Technologies*, **22** (2011), 180-189.

[9] M.J. Dalby, N. Gadegaard, R. Tare, A. Andar, M.O. Riehle, P. Herzyk, C.D.W. Wilkinson and R.O.C. Oreffo, The control of human mesenchymal cell differentiation using nanoscale symmetry and disorder, *Nature Materials*, **6** (2007), 997-1003.

[10] G.P. Dimri, X.H. Lee, G. Basile, M. Acosta, C. Scott, C. Roskelley, E.E. Medrano, M. Linskens, I. Rubelj, O. Pereirasmith, M. Peacocke and J. Campisi, A Biomarker That Identifies Senescent Human-Cells in Culture and in Aging Skin *in-Vivo*, *Proceedings*

of the National Academy of Sciences of the United States of America, **92** (1995), 9363-9367.

[11] D. Docheva, C. Popov, W. Mutschler and M. Schieker, Human mesenchymal stem cells in contact with their environment: Surface characteristics and the integrin system, *Journal of Cellular and Molecular Medicine*, **11** (2007), 21-38.

[12] G. Duque, M. Macoritto and R. Kremer, 1,25(OH)2D3 inhibits bone marrow adipogenesis in senescence accelerated mice (SAM-P/6) by decreasing the expression of peroxisome proliferator-activated receptor gamma 2 (PPARgamma2), *Exp Gerontol*, **39** (2004), 333-338.

[13] A.J. Engler, S. Sen, H.L. Sweeney and D.E. Discher, Matrix elasticity directs stem cell lineage specification, *Cell*, **126** (2006), 677-689.

[14] D. Furlani, W.Z. Li, E. Pittermann, C. Klopsch, L. Wang, A. Knopp, P. Jungebluth, E. Thedinga, C. Havenstein, I. Westien, M. Ugurlucan, R.K. Li, N. Ma and G. Steinhoff, A Transformed Cell Population Derived From Cultured Mesenchymal Stem Cells Has no Functional Effect After Transplantation Into the Injured Heart, *Cell Transplantation*, **18** (2009), 319-331.

[15] S. Gehmert, S. Gehmert, M. Hidayat, M. Sultan, A. Berner, S. Klein, J. Zellner, M. Müller and L. Prantl, Angiogenesis: The role of PDGF-BB on adipose-tissue derived stem cells (ASCs). *Clinical Hemorheology and Microcirculation*. **48** (2011), 5-13.

[16] S. Gehmert, S. Gehmert, X. Bai, S. Klein, O. Ortmann and L. Prantl, Limitation of *in vivo* models investigating angiogenesis in breast cancer, *Clinical Hemorheology and Microcirculation*, **49** (2011), 519-526.

[17] L. Hayflick and P.S. Moorhead, The serial cultivation of human diploid cell strains, *Exp Cell Res*, **25** (1961), 585-621.

[18] B. Hiebl, K. Lutzow, M. Lange, F. Jung, B. Seifert, F. Klein, T. Weigel, K. Kratz and A. Lendlein, Cytocompatibility testing of cell culture modules fabricated from specific candidate biomaterials using injection molding, *Journal of Biotechnology*, **148** (2010), 76-82.

[19] N. Huebsch, P.R. Arany, A.S. Mao, D. Shvartsman, O.A. Ali, S.A. Bencherif, J. Rivera-Feliciano and D.J. Mooney, Harnessing traction-mediated manipulation of the cell/matrix interface to control stem-cell fate, *Nature Materials*, **9** (2010), 518-526.

[20] R. Izadpanah, D. Kaushal, C. Kriedt, F. Tsien, B. Patel, J. Dufour and B.A. Bunnell, Long-term *in vitro* expansion alters the biology of adult mesenchymal stem cells, *Cancer Research*, **68** (2008), 4229-4238.

[21] S.H. Kim, B.M. Lee, S.K. Min, S.U. Song, J.H. Cho, K. Cho and H.S. Shin, Modulation of the heterogeneous senescence of human mesenchymal stem cells on chemically-modified surfaces, *Colloids and Surfaces B-Biointerfaces*, **90** (2012), 36-40.

[22] K.P. Kommareddy, C. Lange, M. Rumpler, J.W.C. Dunlop, I. Manjubala, J. Cui, K. Kratz, A. Lendlein and P. Fratzl, Two stages in three-dimensional *in vitro* growth of tissue generated by osteoblastlike cells, *Biointerphases*, **5** (2010), 45-52.

[23] K.C. Kregel and H.J. Zhang, An integrated view of oxidative stress in aging: Basic mechanisms, functional effects, and pathological considerations, *American Journal of Physiology-Regulatory Integrative and Comparative Physiology*, **292** (2007), R18-R36.

[24] M. Lange, S. Braune, K. Luetzow, K. Richau, N. Scharnagl, M. Weinhart, A.T. Neffe, F. Jung, R. Haag and A. Lendlein, Surface Functionalization of Poly(ether imide) Membranes with Linear, Methylated Oligoglycerols for Reducing Thrombogenicity, *Macromolecular Rapid Communications*, (2012), 1487-1492.

[25] A. Lendlein, M. Behl, B. Hiebl and C. Wischke, Shape-memory polymers as a technology platform for biomedical applications, *Expert Review of Medical Devices*, **7** (2010), 357-379.

[26] W. Li, N. Ma, L.L. Ong, C. Nesselmann, C. Klopsch, Y. Ladilov, D. Furlani, C. Piechaczek, J.M. Moebius, K. Lutzow, A. Lendlein, C. Stamm, R.K. Li and G. Steinhoff, Bcl-2 engineered MSCs inhibited apoptosis and improved heart function, *Stem Cells*, **25** (2007), 2118-2127.

[27] P.J. Lou, M.Y. Chiu, C.C. Chou, B.W. Liao and T.H. Young, The effect of poly (ethylene-co-vinyl alcohol) on senescence-associated alterations of human dermal fibroblasts, *Biomaterials*, **31** (2010), 1568-1577.

[28] A.M. Mackay, S.C. Beck, J.M. Murphy, F.P. Barry, C.O. Chichester and M.F. Pittenger, Chondrogenic differentiation of cultured human mesenchymal stem cells from marrow, *Tissue Engineering*, **4** (1998), 415-428.

[29] K. Mareschi, I. Ferrero, D. Rustichelli, S. Aschero, L. Gammaitoni, M. Aglietta, E. Madon and F. Fagioli, Expansion of mesenchymal stem cells isolated from pediatric and adult donor bone marrow, *Journal of Cellular Biochemistry*, **97** (2006), 744-754.

[30] K. Masutomi, E.Y. Yu, S. Khurts, I. Ben-Porath, J.L. Currier, G.B. Metz, M.W. Brooks, S. Kaneko, S. Murakami, J.A. DeCaprio, R.A. Weinberg, S.A. Stewart and W.C. Hahn, Telomerase maintains telomere structure in normal human cells, *Cell*, **114** (2003), 241-253.

[31] R. McBeath, D.M. Pirone, C.M. Nelson, K. Bhadriraju and C.S. Chen, Cell shape, cytoskeletal tension, and RhoA regulate stem cell lineage commitment, *Developmental Cell*, **6** (2004), 483-495.

[32] R.J. McMurray, N. Gadegaard, P.M. Tsimbouri, K.V. Burgess, L.E. McNamara, R. Tare, K. Murawski, E. Kingham, R.O.C. Oreffo and M.J. Dalby, Nanoscale surfaces for the long-term maintenance of mesenchymal stem cell phenotype and multipotency, *Nature Materials*, **10** (2011), 637-644.

[33] E.J. Moerman, K. Teng, D.A. Lipschitz and B. Lecka-Czernik, Aging activates adipogenic and suppresses osteogenic programs in mesenchymal marrow stroma/stem cells: The role of PPAR-gamma2 transcription factor and TGF-beta/BMP signaling pathways, *Aging Cell*, **3** (2004), 379-389.

[34] C. Nesselmann, N. Ma, K. Bieback, W. Wagner, A. Ho, Y.T. Konttinen, H. Zhang, M.E. Hinescu and G. Steinhoff, Mesenchymal stem cells and cardiac repair, *Journal of Cellular and Molecular Medicine*, **12** (2008), 1795-1810.

[35] C. Nombela-Arrieta, J. Ritz and L.E. Silberstein, The elusive nature and function of mesenchymal stem cells, *Nature Reviews Molecular Cell Biology*, **12** (2011), 126-131.

[36] L. Ou, W. Li, Y. Liu, Y. Zhang, S. Jie, D. Kong, G. Steinhoff and N. Ma, Animal models of cardiac disease and stem cell therapy, *The Open Cardiovascular Medicine Journal*, **4** (2010), 231-239.

[37] B.F. Pierce, E. Pittermann, N. Ma, T. Gebauer, A.T. Neffe, M. Holscher, F. Jung and A. Lendlein, Viability of Human Mesenchymal Stem Cells Seeded on Crosslinked Entropy-Elastic Gelatin-Based Hydrogels, *Macromolecular Bioscience*, **12** (2012), 312-321.

[38] M.F. Pittenger, A.M. Mackay, S.C. Beck, R.K. Jaiswal, R. Douglas, J.D. Mosca, M.A. Moorman, D.W. Simonetti, S. Craig and D.R. Marshak, Multilineage potential of adult human mesenchymal stem cells, *Science*, **284** (1999), 143-147.

[39] K. Stenderup, J. Justesen, C. Clausen and M. Kassem, Aging is associated with decreased maximal life span and accelerated senescence of bone marrow stromal cells, *Bone*, **33** (2003), 919-926.

[40] R. Tzoneva, B. Seifert, W. Albrecht, K. Richau, T. Groth and A. Lendlein, Hemocompatibility of poly(ether imide) membranes functionalized with carboxylic groups, *Journal of Materials Science-Materials in Medicine*, **19** (2008), 3203-3210.

[41] M. Ugurlucan, C. Yerebakan, D. Furlani, N. Ma and G. Steinhoff, Cell sources for cardiovascular tissue regeneration and engineering, *The Thoracic and Cardiovascular Surgeon*, **57** (2009), 63-73.

[42] W. Wagner, P. Horn, M. Castoldi, A. Diehlmann, S. Bork, R. Saffrich, V. Benes, J. Blake, S. Pfister, V. Eckstein and A.D. Ho, Replicative senescence of mesenchymal stem cells: A continuous and organized process, Public Library of Science One, **3** (2008), e2213.

[43] W. Wagner, S. Bork, P. Horn, D. Krunic, T. Walenda, A. Diehlmann, V. Benes, J. Blake, F.X. Huber, V. Eckstein, P. Boukamp and A.D. Ho, Aging and Replicative Senescence Have Related Effects on Human Stem and Progenitor Cells, *Public Library of Science One*, **4** (2009), e5846.

[44] Y.H. Wan, L.W. Chong and R.M. Evans, PPAR-gamma regulates osteoclastogenesis in mice, *Nature Medicine*, **13** (2007), 1496-1503.

[45] W.W. Wang, W.Z. Li, L.L. Ou, E. Flick, P. Mark, C. Nesselmann, C.A. Lux, H.H. Gatzen, A. Kaminski, A. Liebold, K. Luetzow, A. Lendlein, R.K. Li, G. Steinhoff and N. Ma, Polyethylenimine-mediated gene delivery into human bone marrow mesenchymal stem cells from patients, *Journal of Cellular and Molecular Medicine*, **15** (2011), 1989-1998.

[46] T.L. Yew, F.Y. Chiu, C.C. Tsai, H.L. Chen, W.P. Lee, Y.J. Chen, M.C. Chang and S.C. Hung, Knockdown of p21(Cip1/Waf1) enhances proliferation, the expression of stemness markers, and osteogenic potential in human mesenchymal stem cells, *Aging Cell*, **10** (2011), 349-361.